

A Plug-and-Play Physical Motion Restoration Approach for In-the-Wild High-Difficulty Motions

Youliang Zhang^{1*} Ronghui Li^{1*} Yachao Zhang¹
 Liang Pan² Jingbo Wang² Yebin Liu¹ Xiu Li^{1†}
¹Tsinghua University, China ²Shanghai AI Laboratory

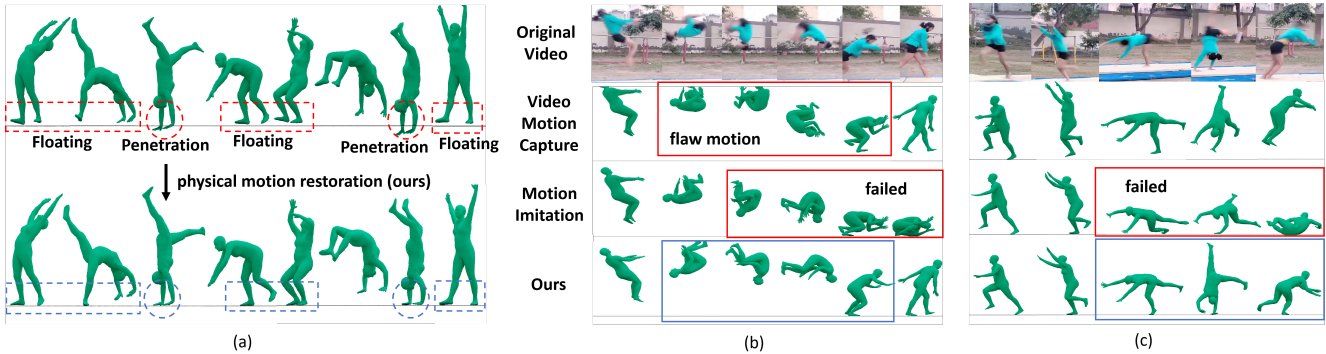


Figure 1. **Illustration of motivation and two main challenges.** (a) Our method effectively enhances the physical plausibility of video-captured motions, even handling high-difficulty motions like backflips. (b) highlights the challenging movements in the original video lead to flawed motion estimated by current video motion capture algorithms, where the current motion imitation model fails to restore overly degraded flawed motions. (c) demonstrates that even when video motion capture provides reasonable reference motions, existing motion imitation techniques still fail to track complex motions.

Abstract

Extracting physically plausible 3D human motion from videos is a critical task. Although existing simulation-based motion imitation methods can enhance the physical quality of daily motions estimated from monocular video capture, extending this capability to high-difficulty motions remains an open challenge. This can be attributed to some flawed motion clips in video-based motion capture results and the inherent complexity in modeling high-difficulty motions. Therefore, sensing the advantage of segmentation in localizing human body, we introduce a mask-based motion correction module (MCM) that leverages motion context and video mask to repair flawed motions, producing imitation-friendly motions; and propose a physics-based motion transfer module (PTM), which employs a pretrain and adapt approach for motion imitation, improving physical plausibility with the ability to handle in-the-wild and challenging motions. Our approach is designed as a plug-and-play module to physically refine the video motion capture results, including high-difficulty in-the-wild motions. Finally, to validate our approach, we collected a challenging in-the-wild test set to

establish a benchmark, and our method has demonstrated effectiveness on both the new benchmark and existing public datasets. <https://physicalmotionrestoration.github.io/>

1. Introduction

Physical plausible 3D human motion is in high demand across various fields, including virtual reality, game, animation industries, and academic research on virtual humans and robotics [4, 7, 13, 27, 32, 38, 46, 62, 64, 77]. With technological advancements, monocular video-based motion capture algorithms provide a fast and convenient pipeline for obtaining 3D motion closely aligned with video. However, these methods inherently lack dynamic modeling, resulting in significant physical unrealisms such as floating, foot sliding, self-intersections, and ground penetration, things get worse when facing high-difficulty motions.

To enhance physical realism, some methods use dynamic equations and train a network to predict physical parameters [10, 24, 59, 70]. However, these methods often struggle to improve motion plausibility due to oversimplified dynamic equations. Other methods [9, 12, 51, 73] use physical-simulation-based motion imitation as a post-processing module, learning motion control policy to imitate the reference motion (video motion capture results) in

*Equal contribution

†Corresponding author

a simulated physical environment. With high-quality reference motions, these methods improve the physical realism of daily motions such as walking, running, and jumping. However, they can not handle high-difficulty movements like gymnastics and martial arts. Regarding this, we aim to extend the physical restoration ability of motion imitation in high-difficulty and in-the-wild motions, meeting broader requirements for motion asset acquisition.

Reviewing the characteristics of high-difficulty motions, they often involve rapid movement, extreme poses, skilled force control, and follow a long-tail distribution in existing datasets. This presents two major challenges for existing motion imitation methods to enhance the physical plausibility of complex motions within a physical simulation environment: (1) **Flawed Reference Motions**: As shown in Fig 1(b), even the state-of-the-art video motion capture algorithms estimate flawed motions when facing challenging movements. Such brief disruptions can easily cause failures in the motion imitation process and are obvious in the human senses. (2) **Inherent Imitation Complexity**: The long-tail distribution of high-difficulty motions and their complex force control skills make it challenging for current motion imitation methods to track high-difficulty motions, shown in Fig 1(c). Moreover, a single controller struggles to generalize across a diverse range of high-difficulty movements, facing catastrophic forgetting issues, where rapid loss of old knowledge occurs when learning new skills [33].

To solve the issue of **flawed reference motion**, we propose a mask-conditioned correction module (MCM). Due to the blurred frames caused by rapid and extreme poses, video motion capture algorithms struggle to localize body parts accurately when facing high-difficulty motions. Notably, the nature of segmentation methods to distinguish the foreground and background mitigates the effects of blurred frames, allowing them to define an approximate range of body. Also, the flaw motion occurs over a short time and is surrounded by rich motion contexts, making segmentation-guided interpolation and replacement of flaw motion possible. We first leverage a large visual semantic segmentation model [20] to obtain human segmentation masks of the input video. Then, guided by segmentation masks and reference motion context, we regenerate context-consistent and imitation-friendly motions to replace the flawed motion, allowing accurate and complete motion imitation.

To tackle the **inherent imitation complexity** of diverse challenging movements, we propose a Physics-based Motion Transfer Module (PTM) consisting of a pre-trained imitation controller and a test time adaptation strategy (TTA). Utilizing the trial-and-error nature of reinforcement learning and pre-trained motion prior, we targeted adapting our network to current motion in test time, naturally addressing the long-tail distribution and domain gap issues by parameter updating. To better achieve complex force control, our

TTA contains unique imitation settings for adaptation to facilitate tracking the noisy yet challenging motions captured from videos. The pretrain and adapt pattern of PTM greatly improves the imitation ability, allowing the successful physical restoration of in-the-wild and high-difficulty motions.

Through our proposed novel MCM and PTM, we successfully address the failure issues of flaw motion and complex motion simulation, achieving physical authenticity restoration in high-difficulty motions while faithfully retaining the original movements. It is worth mentioning that without additional training, our method can be conveniently integrated into any video motion capture method, directly repairing in-the-wild and high-difficulty motions.

To validate the effectiveness of our proposed motion restoration method, we collected 206 high-difficulty motion videos entirely in the wild, including activities such as rhythmic gymnastics, taekwondo, and yoga. Our method demonstrated strong performance on this in-the-wild test set, which is significantly more challenging than the training set, further proving the effectiveness of our approach.

Our contributions can be summarized as follows:

- We propose a plug-and-play motion restoration method that enhances the physical realism of motions captured from monocular video. It can be integrated with existing motion capture algorithms to improve the efficiency of obtaining high-quality 3D motion.
- We introduced an MCM for correcting short-term flawed motions, producing consistent and imitation-friendly motions for physical restoration.
- We introduced a PTM with a pretrain and adapt motion imitation pattern, allowing the physical restoration of high-difficulty and in-the-wild motions.
- We collected a challenging in-the-wild test set to establish a benchmark, and our method demonstrates effectiveness on both the new benchmark and existing public datasets.

2. Related Work

2.1. Video Motion Capture

Most works for video motion capture are to recover the parameters of a parametric human model [2, 6, 11, 17, 21, 28, 30, 36, 49, 54, 58]. Recently, many methods have started to consider moving cameras. TRACE [55] and WHAM [53] propose regressing per-frame poses and translations. SLAHMR [71] and PACE [22] integrate SLAM [56, 57] with motion priors [45] into the optimization framework. TRAM [67] leverages the scene background to derive motion scale. GVHMR [50] estimates human poses in a novel Gravity-View coordinate system. While these methods achieve significant success in reconstructing high-difficulty motions from videos, they suffer from serious physical issues and occasionally experience flawed motions when facing complex movements. Our proposed physical motion

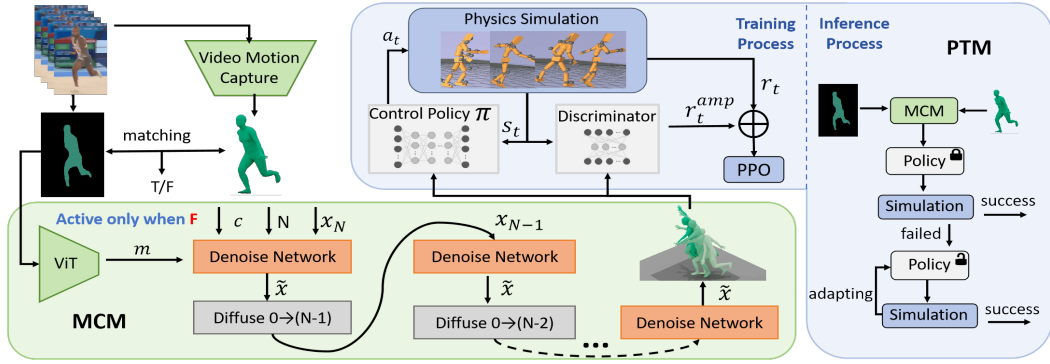


Figure 2. **Illustration of our proposed method.** If no mismatch is detected between the human mask and noise motion, the correction process will be skipped, and our PTM directly takes the noise motion as input. When failed with challenge motions, our PTM will adapt the policy to the current motion and update the network parameters until success or reach a certain step threshold.

restoration method effectively addresses these problems.

2.2. Motion Imitation

The physical constraints provided by simulation environments give simulated characters a clear advantage in generating lifelike human movements [1, 8, 12, 35, 39–44, 63, 66, 68]. Early works focused on small-scale task-specific scenarios and are difficult to generalize to other domains. With the advancements in motion generation technology [29], training policies to imitate large-scale motion datasets show broader application potential [44]. Researchers improve motion simulation quality by leveraging techniques such as hybrid expert policies [69], differentiable simulation [47], and external forces [72]. ScaDiver [69] extended the hybrid expert strategy to the CMU motion capture dataset. Unicorn [65] demonstrated qualitative results in imitation and transfer tasks. MoCapAct [61] learn a single-segment expert policy on the CMU dataset. UHC [31] successfully imitated 97% of the AMASS dataset, and recently, PHC [33, 34] enabled a single policy to simulate almost the entire AMASS dataset while allowing recovery from falls. However, these methods rely heavily on the quality of reference motions and are largely confined to locomotion tasks. Simulating in-the-wild and high-difficulty motions is still challenging, where our proposed PTM provides a possible solution.

2.3. Physics informed Video Motion Capture

Many researchers attempt to introduce physics into video motion capture. Some methods [10, 15, 23, 52, 59] leverage neural networks to estimate physical parameters for motion capture and introduce the kinematic constrains to enhance the physical plausibility. LEMO [75] uses motion smoothness prior and physics contact friction term. Xie *et al.* [70] propose differentiable physics-inspired objectives with contact penalty. IPMAN [59] exploits intuitive-physics terms to incorporate physics. Li *et al.* [24] enhanced the learning process by incorporating 3D supervision. These methods typically require hard-to-obtain 3D annotations and overly simplify dynamic equations, struggling with generalization to out-of-distribution motions. There are also

methods combine motion imitation to enhance the physical plausibility, they treat the captured motion as a reference and predict the physical simulation forces with a controller [12, 73, 78]. DiffPhy [9] uses a differentiable physics simulator during inference. PhysCap [51] uses a numerical optimization framework with soft physical constraints. SimPoE [73] integrates image-based kinematic inference and physics-based dynamics modeling. However, these methods typically require careful tuning of control parameters and are sensitive to different motion types [15]. This sensitivity makes it challenging to generalize to in-the-wild high-difficulty motions, limiting real-world applications. Recently, PhysPT [76] proposed a pre-trained physics-aware transformer to learn human dynamics in a self-supervised manner. However, it lacks an understanding of the distribution and physical rules of high-difficulty motions, necessitating additional physical priors of complex motions, which is challenging due to data scarcity. In contrast, our approach is designed to restore high-difficulty and in-the-wild motions while maintaining their original motion pattern.

3. Physics-based Motion Restoration

Our method takes video-captured motion as reference motions and focuses on restoring their physical realism while preserving original motion patterns. The motion representation x_t consists of joint position $p_t \in \mathbb{R}^{J \times 3}$ and rotation $\theta_t \in \mathbb{R}^{J \times 6}$ [79], compatible with SMPL format [28]. J means the joint number of the humanoid. The reference velocities q_t is also considered, which consists of the linear $v_t \in \mathbb{R}^{J \times 3}$ and angular $\omega_t \in \mathbb{R}^{J \times 6}$ velocity. An overview of our method is provided in Fig 2. Given the reference motion (video motion capture results) and corresponding video, our MCM detects and corrects the flawed motion. Our PTM inputs the corrected motion and performs physical restoration by motion imitation. In PTM, a pre-trained controller and a carefully designed adaptation strategy are well-cooperated to solve the dynamics of a single motion. This pre-train and adapt pattern makes our PTM perform well in tracking high-difficulty and in-the-wild motions.

3.1. Preliminaries

Motion Imitation. The problem of controlling a humanoid to follow a reference motion sequence can be formulated as a Markov Decision Process, defined by the tuple $M = \langle S, A, P_{\text{physics}}, R, \gamma \rangle$, which consists of states, actions, transition dynamics, reward, and a discount factor. At step t , agent samples an action \mathbf{a}_t from the policy $\pi_{\text{PTM}}(\mathbf{a}_t | \mathbf{s}_t)$ based on the current state \mathbf{s}_t , and the environment responds with the next state \mathbf{s}_{t+1} and a reward r_t . Proximal Policy Optimization [48] is used to optimize the policy π_{PTM}^* by maximize the expected discounted return $\mathbb{E} \left[\sum_{t=1}^T \gamma^{t-1} r_t \right]$. The state \mathbf{s}_t consists of positions, rotations, and linear and angular velocities of humanoid, as well as the next frame information \mathbf{g}_t . We define \mathbf{g}_t as the difference between the current frame and next frame reference motion [33, 74]. The action \mathbf{a}_t specifies the target humanoid joint angles for the controller at each degree of freedom (DoF). Given an action and current motion \mathbf{x}_t and velocity \mathbf{q}_t , the torque to be applied is computed as:

$$\boldsymbol{\tau}^i = \mathbf{k}_p^i (\mathbf{a}_t^i - \mathbf{x}_t^i) - \mathbf{k}_d^i \mathbf{q}_t^i, \quad (1)$$

where i means joint DoF index, \mathbf{k}_p and \mathbf{k}_d are manually-specified gains. Our policy π_{PTM} is constructed with multilayer perceptions and ReLU functions. A discriminator from AMP [43] is used to predict whether a given state \mathbf{s}_t and action \mathbf{a}_t is sampled from the demonstrations M or generated by policy π_{PTM} . The reward consists of a reconstruction reward r_t^g to follow the reference motion, a style reward r_t^{amp} produced by the amp discriminator, and an energy penalty reward r_t^{energy} [41] to prevents motion jitter.

$$r_t = r_t^g + r_t^{\text{amp}} + r_t^{\text{energy}}. \quad (2)$$

Motion Diffusion Model. The diffusion model consists of a forward diffusion process that progressively adds noise to the clean data and a reverse diffusion process trained to reverse this process. The forward diffusion process introduces noise for N steps formulated using a Markov chain:

$$q(\mathbf{x}_{1:N} | \mathbf{x}_0) := \prod_{n=1}^N q(\mathbf{x}_n | \mathbf{x}_{n-1}), \quad (3)$$

Reverse process employs a learnable network f_θ to denoise.

3.2. Mask-conditioned Motion Correction Module

Flaw motions in video capture results manifest as incoherent frames within the motion sequence inconsistent with the surrounding motion context. Although such brief disruptions have a minimal impact on metrics, they can easily cause failures in the physics simulation process and are obvious in the human senses. To address this issue, our MCM first detects flawed motion and then regenerates the flawed

motion segment guided by the motion context and human mask signals, ultimately replacing the flawed motion.

Mismatch Detection. Given the reference motion and its corresponding video, we project the 3D positions of the reference motion into 2D camera coordinates. Also, an object detection algorithm is used to extract the corresponding 2D keypoints from the video. Using the Object Keypoint Similarity (OKS) algorithm, we compute the matching degree between the two sets of keypoints and obtain a similarity score sequence. Frames with a similarity score below a certain threshold will be flagged as flaw motion.

$$OKS = \frac{\sum_i \exp(-d_i^2 / 2\epsilon_i^2) \delta(v_i > 0)}{\sum_i \delta(v_i > 0)} \quad (4)$$

where v_i represents the visibility flag, ϵ_i denotes the scale factor, and d_i is the distance difference between the projection and the detection results. Additionally, segmentation algorithms can also be used to detect flaw motion. We project the SMPL-generated mesh onto the 2D plane and treat it as a set of pixel points. The matching similarity can be calculated by determining the proportion of projected mesh points that are contained within the human mask.

Motion Correction Goal Design. Unlike traditional motion in-between methods, the goal of MCM is to replace flawed motions in the reference sequence based on contextual information, ensuring that the corrected motion is smooth and reasonable. Thus, we focus on the model’s ability to fill temporal gaps. Since the input is motion captured from video, ensuring the generated motion remains consistent with the original video content is crucial. Therefore, we use the human mask obtained from segmentation as a conditional signal to guide the in-between process.

Mask-conditioned Diffusion In-betweening. Given a reference motion sequence $\mathbf{x} \in \mathbb{R}^{N \times D}$, the segmented human mask (obtained from SAM [20]) $\mathbf{m} \in \mathbb{R}^{N \times w \times h}$, and a keyframe signal $\mathbf{c} \in \mathbb{R}^N$ (mismatch detection results to identifies flaw motion), this module correct the reference motion by replacing mismatched motion frames. We employ a pre-trained Vision Transformer (ViT) as the mask feature extractor to capture rich human pose information from the segmentation mask. The mask combined with the motion context is used as the condition of the motion diffusion model. Following [3, 18], we concatenate the resulting sample, keyframe signal, and mask features as model input to inform the generation model with condition signal.

Training process. A random motion segment, selected at a random sequence position, is chosen as the generation target. Our model is trained to reconstruct this segment. Both keyframe conditioning signals \mathbf{c} and mask conditioning signal \mathbf{m} are set to \emptyset for 10% of training data to make our model suited for unconditioned motion generation.

3.3. Physics-based Motion Transfer Module

Our PTM consists of a pre-trained imitation controller and a test time adaptation strategy. The controller, as defined in the Motion Imitation section, obtains basic motion imitation ability with substantial motion prior. The TTA strategy (with a set of adaptation settings) is carefully designed to adapt the controller to explore a single specific motion, solving the dynamic modeling of noised high-difficulty motion. Compared to previous methods, the pretrain and adapt pattern avoids limiting the model to a specific data domain. It models the dynamics for a single motion based on the normal prior, significantly enhancing the ability to handle out-of-domain and high-difficulty motions.

Imitation Controller Pre-training. Acquiring as much motion prior knowledge as possible during the pre-training phase is essential to accelerate the adaptation process. Therefore, we perform pre-training on 4 datasets: AMASS [37], Human3.6M [16], AIST++ [25, 60], and Motion-X [26] kungfu subset. The pre-training phase employs strict reconstruction rewards and early termination conditions.

RL-based Test Time Adaptation. With a pre-trained imitation controller, rich motion priors open up the possibility for rapid adaptation during test time. Utilizing the trial-and-error nature of reinforcement learning, we propose RL-based test time adaptation, which involves performing a limited number of experiment steps on the current test data under specific adaptation settings (updating network parameters). Each motion sequence is treated as an individual instance, and the adaptation is performed for each instance independently. This method is particularly useful when dealing with high-difficulty and low-quality motions. The following designs are used in the adaptation process.

Relative Reward. The captured reference motion contains jitter or fault roots with error accumulation, making constructing a full reconstruction reward detrimental. Therefore, in the adaptation process, we designed a relative reward r_t^g that neglects the absolute root position, maintaining global orientation and translation through explicit guidance from rotation and implicit guidance from velocity. The relative reward is formulated as:

$$r_t^g = e^{w_p \|rela(\hat{\mathbf{p}}_t) - rela(\mathbf{p}_t)\|} + e^{w_r \|\hat{\boldsymbol{\theta}}_t \ominus \boldsymbol{\theta}_t\|} + e^{w_v \|\hat{\mathbf{v}}_t - \mathbf{v}_t\|} + e^{w_\omega \|\hat{\boldsymbol{\omega}}_t - \boldsymbol{\omega}_t\|}, \quad (5)$$

where $\hat{\mathbf{p}}_t$ means the joint position of reference motion, $rela()$ means to ignore the gravity axis part of root joints. \ominus means rotation difference and w is weights factor.

Early Termination. In high-difficulty motion tracking, there is a large displacement between humanoid and reference motion, as reference motion often involves frequent floating and penetration. This phenomenon makes defining when an adaptation step should be terminated challenging, which is crucial for adaptation efficiency and prevent-

ing undesirable behaviors. Therefore, we design a relative termination condition by calculating each joint’s mean relative distance between humanoid and reference motion. One adaptation step will be terminated when the distance exceeds threshold d_{term} . We also introduce termination condition \mathcal{F}_t^h and \mathcal{F}_t^c based on joint height and ground contact to consider falls and erroneous contacts occur. The full termination \mathcal{F}_t is defined below, a smaller threshold d_{term} indicating a stricter adherence to reference motion.

$$\mathcal{F}_t = \left(\frac{1}{J} \sum_{i=1}^J \|rela(\hat{\mathbf{p}}_t^i) - rela(\mathbf{p}_t^i)\| > d_{term} \right) \vee \mathcal{F}_t^h \vee \mathcal{F}_t^c \quad (6)$$

Residual Force. During the test-time adaptation phase, we introduce residual forces [72] to compensate for the dynamics mismatch. This is important because complex motions often involve airborne flips and jumps (commonly seen in gymnastics and martial arts), which frequently rely on elastic trampolines and mats for execution. The use of external forces is necessary to account for the absence of these environmental conditions in our simulations.

4. Experimental Results and Analysis

4.1. Datasets

We use four datasets to train our model: AMASS [37], Human3.6M [16], AIST++ [25, 60], and Motion-X [26] kungfu subset. AIST++ contains 5 hours of diverse dance motions, Motion-X is a huge motion generation dataset and its kungfu subset contains complex kungfu motions over 1k clips. We perform our evaluations on the test set of AIST++, EMDB [19], and kungfu. Sequences involving human-object interactions are removed for all datasets.

We collected 206 high-difficulty motion videos from YouTube, including rhythmic gymnastics (floor, ball, ribbon), dance (breakdancing, ballet, yoga), and martial arts (kungfu, taekwondo). We use these videos as in-the-wild data for evaluation. Compared to the previously mentioned datasets, these videos contain more complex motions, posing greater challenges for physics-based motion repair tasks. These data can also be used to evaluate the generalization capabilities of 3D human motion recovery methods, and we will make them publicly available.

4.2. Metrics

Following the latest method [50, 53, 67], we evaluate camera-coordinate metrics using the widely used MPJPE, Procrustes-aligned MPJPE (PA-MPJPE), Per Vertex Error (PVE), and Acceleration error (Accel). For world-coordinate metrics, we divide the global sequences into shorter segments of 100 frames aligning each segment with GT like GVHMR [50]. We then report the World-aligned Mean Per Joint Position Error (WA-MPJPE₁₀₀), the World

MPJPE (W-MPJPE₁₀₀), and the whole sequence for Root Translation Error (RTE, in %). In addition, we designed a benchmark to assess physical realism and motion reconstruction fidelity. This evaluation metric does not require 3D annotated data and is suitable for reflecting the model’s generalization capability on in-the-wild motions.

Physical realism. 1) **Self-Penetration (SP)** measures self-intersection severity. 2) **Ground-Penetration (GP)** measures ground penetration 3) **Float** measures meshes floating above the plane. 4) **Foot-Skate (FS)** measures foot sliding, we find feet that contact the ground in adjacent frames and calculate their average horizontal differences.

2D Similarity. We utilize object segmentation and 2D keypoint detection methods to annotate our in-the-wild test set and design metrics for 2D and 3D Similarity. 1) **2D Keypoint OKS.** We project the 3D motion onto 2D space and compute the Object Keypoint similarity with the 2D keypoints; a higher similarity indicates better restoration of the estimated 3D motion. 2) **Mask-Pose Similarity (MPS).** We project the 3D human mesh into the 2D camera plane and calculate the ratio of mesh points that fall within the segmented human mask. A larger ratio signifies higher motion restoration and a more accurate human shape estimation.

4.3. Implementation details

It takes around 2-3 days to get our pre-trained PTM with a single NVIDIA A100 GPU. During inference, restoring normal motions (such as running and jumping) requires fewer adaptation steps (less than 500) or may not require any adaptation at all. In contrast, restoring high-difficulty motions (such as continuous rolls and aerial maneuvers) necessitates between 2,000 and 4,000 steps, depending on the complexity of the motion and the quality of the reference action. We adopt the motion diffusion model GMD with UNet architecture as our in-between baseline [5, 14]. For more implementation details, please refer to the Appendix.

4.4. Comparison with the State-of-the-Art

We selected two state-of-the-art (SOTA) video motion capture methods, TRAM [67] and GVHMR [50], and SOTA physical informed method PhysPT [76] for comparison. The comparison results are presented in Table 1.

For **world coordinate** metrics, our method outperforms the original motions in most cases. This improvement stems from the direct relationship between the world coordinate system and physical space. Particularly in the EMDB dataset, where prolonged displacement leads to the accumulation of errors in local perspectives over time and space, our method effectively mitigates these issues, resulting in improvements in world coordinate metrics. Previous simulation methods typically emphasized perfect tracking of reference motions, focusing more on imitation rather than restoration. Consequently, when there is a significant de-

viation in the root position along the gravity axis, these methods often fail due to the influence of gravity, especially when attempting to imitate complex or flawed motions. In contrast, our approach prioritizes repair, utilizing a unique PTM that enables stable tracking of high-difficulty motions.

For 3D motion restoration in the **camera coordinate**, our method shows minor discrepancies from the original motions in both the Kungfu and AIST++ datasets. This can be attributed to two main reasons: 1) Our method uses noisy motions as input without knowledge of the GT motions, which inherently disadvantages us. 2) Our repair approach models directly in physical space without considering camera parameters, making it challenging to achieve perfect restoration from specific camera viewpoints. Despite these challenges, our results on the EMDB dataset exhibit slight improvements compared to the original motions. This is because our method accounts for the physical space and offers a better understanding of long-term global trajectory movements, whereas noisy motions accumulate errors due to changes in time and spatial position.

Regarding **2D similarity**, the repaired motions in the Kungfu dataset show slight improvements over the original motions. This is due to current video motion capture methods being prone to brief flaw motions when dealing with complex motions, which become more pronounced when projected onto 2D images. Our MCM replaces flaw motion based on the human masks and motion context, enhancing the 2D restoration of the repaired motions.

In terms of **physical authenticity** metrics, our method successfully restored the physical realism of motions, resulting in significant improvements in ground penetration, foot sliding, and floating. Our method keeps the ground penetration for all datasets below 0.5; notably, for the EMDB dataset, we reduced the ground penetration from as high as 82 to 0.24. This is attributed to the long-term global trajectory changes, where the errors in the gravity axis accumulate along movements, leading to severe ground penetration and floating. For all three datasets, our method reduces the self-penetration by over 50%. In the Kungfu dataset, we successfully lowered the self-penetration of GVHMR from 0.079 to 0.018. Furthermore, foot sliding also shows consistent improvement for all datasets, largely due to the presence of friction in the physical environment. While motion simulation offers inherent advantages, our differentiation from other physics-based simulation methods lies in the ability to track in-the-wild and complex motions.

4.5. Qualitative Evaluation

In Figure 3, we select high-difficulty in-the-wild motions for visualization and illustrate a comparison against SOTA techniques. GVHMR captures human motions from video and acts as a noise motion generator for PhysPT, PHC+ [34], and our methods. GVHMR successfully captures hu-

Datasets	Method	World Coordinate			Camera Coordinate			2D Similarity			Physical Authenticity			
		WA-MJE ↓	W-MJE ↓	RTE ↓	MPJPE ↓	PA-MPJPE ↓	PVE ↓	Accel ↓	OKS ↑	MPS ↑	SP ↓	GP ↓	Float ↓	FS ↓
AIST++	PhysPT [76] CVPR'24	139.974	218.344	9.307	97.143	68.026	115.007	8.406	0.932	0.778	–	7.677	21.348	2.432
	TRAM [67] ECCV'25	<u>106.197</u>	<u>159.520</u>	9.433	91.809	64.024	107.334	7.727	0.945	0.786	0.150	20.557	489.984	2.350
	TRAM+PhysPT	136.828	218.335	6.510	93.570	67.657	110.989	8.601	0.903	0.757	–	4.079	22.688	2.066
	TRAM+Ours	106.151	157.724	8.962	93.954	67.009	<u>110.245</u>	8.383	0.953	0.787	<u>0.046</u>	<u>0.499</u>	1.974	0.586
	GVHMR [50] SIGGRAPH Asia'24	124.434	197.287	<u>5.083</u>	93.548	<u>65.245</u>	111.548	6.850	0.965	0.790	0.072	12.390	71.190	2.232
Kungfu	GVHMR+PhysPT	182.120	281.093	6.760	143.612	78.791	169.827	8.601	0.905	0.764	–	4.978	27.052	2.468
	GVHMR+Ours	123.365	193.792	4.850	94.037	67.075	112.215	<u>7.302</u>	<u>0.963</u>	0.806	0.046	0.498	<u>1.982</u>	<u>0.587</u>
	PhysPT [76] CVPR'24	135.652	217.131	7.907	128.553	57.458	124.852	12.162	0.919	0.765	–	23.630	94.647	10.955
	TRAM [67] ECCV'25	113.354	209.664	7.539	84.610	<u>55.735</u>	<u>101.079</u>	11.872	0.925	0.761	0.136	4.320	40.924	2.574
	TRAM+PhysPT	174.394	344.192	7.752	119.675	60.467	141.917	12.912	0.916	0.713	–	3.193	21.653	1.146
EMDB	TRAM+Ours	113.284	193.673	7.211	79.493	57.714	91.636	12.626	0.931	<u>0.775</u>	<u>0.077</u>	0.239	5.714	<u>0.259</u>
	GVHMR [50] SIGGRAPH Asia'24	106.763	204.495	<u>4.868</u>	96.316	54.748	113.218	11.630	0.958	0.765	0.079	10.368	43.401	2.217
	GVHMR+PhysPT	211.972	344.590	8.605	97.270	55.923	112.178	14.988	0.902	0.696	–	3.189	26.097	1.774
	GVHMR+Ours	<u>109.986</u>	<u>198.090</u>	4.699	97.995	57.061	112.868	12.234	<u>0.953</u>	0.792	0.018	<u>0.290</u>	<u>6.240</u>	0.257
	PhysPT [76] CVPR'24	285.464	741.967	10.838	264.547	40.952	307.372	5.9063	0.956	0.793	–	1.855	21.144	2.738
EMDB	TRAM [67] ECCV'25	230.633	322.495	3.162	266.600	38.474	305.433	5.546	0.947	0.792	0.073	199.710	161.200	17.373
	TRAM+PhysPT	358.803	881.275	11.627	256.744	40.619	<u>298.817</u>	6.791	0.908	0.767	–	2.382	11.686	1.985
	TRAM+Ours	224.038	312.028	2.074	263.955	40.396	295.395	6.194	0.949	0.797	0.045	<u>1.415</u>	<u>4.562</u>	1.482
	GVHMR [50] SIGGRAPH Asia'24	<u>109.104</u>	<u>274.941</u>	<u>1.960</u>	252.159	<u>38.112</u>	316.509	<u>5.870</u>	<u>0.954</u>	<u>0.801</u>	<u>0.006</u>	82.266	510.298	0.693
	GVHMR+PhysPT	781.128	1491.893	14.588	<u>251.277</u>	50.333	303.236	6.652	0.916	0.751	–	0.983	9.924	<u>0.494</u>
GVHMR+Ours	91.153	261.579	1.180	249.127	37.897	313.925	6.694	0.948	0.807	0.002	0.248	3.632	0.173	

Table 1. **Evaluation on multiple video motion capture dataset.** Since our method is based on physical simulation, we filtered these datasets and removed the human-object interaction scenes. WA-MJE and W-MJE mean WA-MPJPE₁₀₀ and W-MPJPE₁₀₀ separately.

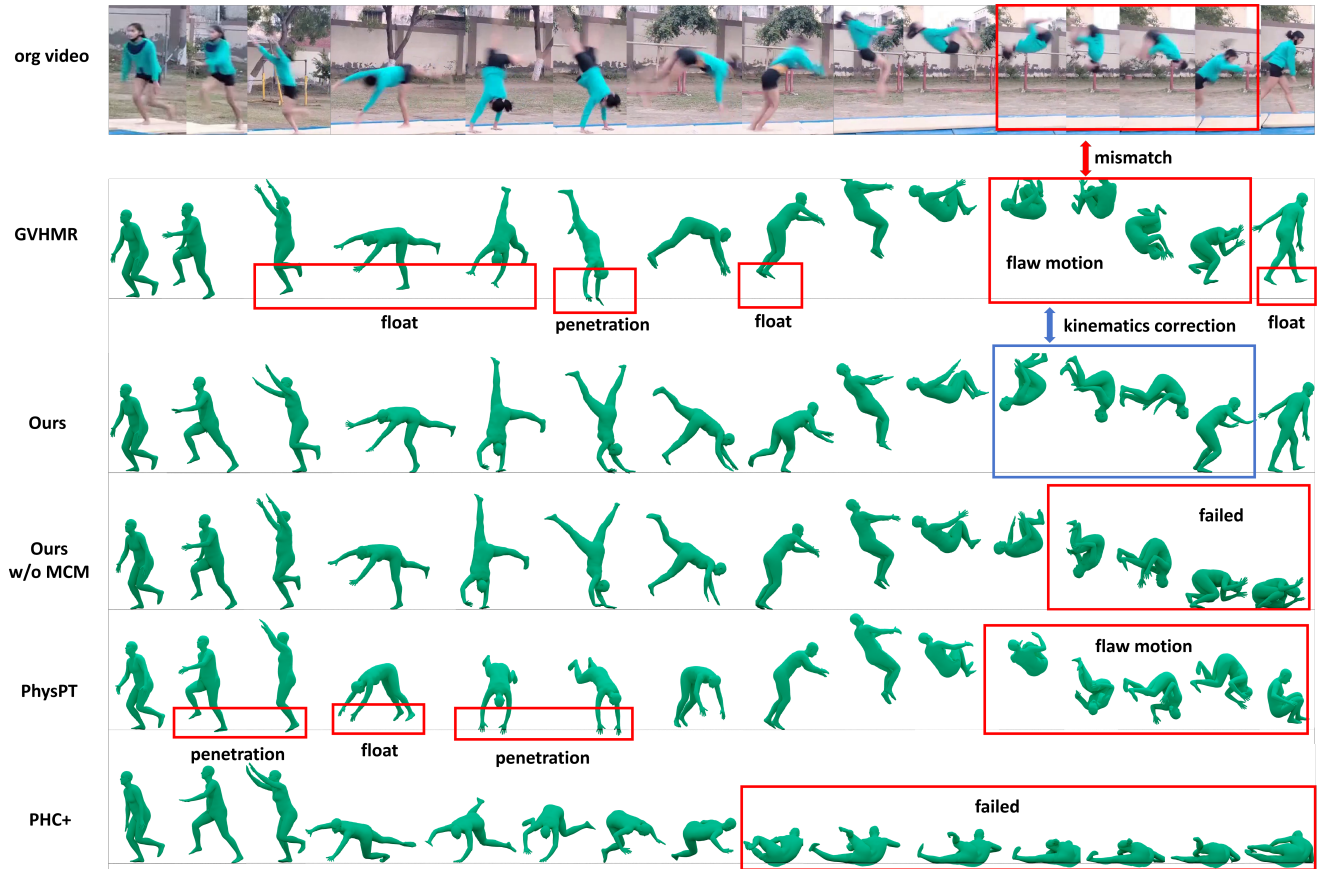


Figure 3. **Qualitative comparison with state-of-the-art method.**

man motion from a monocular camera, yet the resulting motion exhibits significant physical issues such as floating and penetration. Additionally, it manifests short-term flawed motion when faced with more complex movements. Due to

simplified physical rules and the unawareness of the high-difficulty motion distribution, PhysPT faces challenges in both physical repair and preservation of the original motion when dealing with complex motions. Moreover, it is inf-

Method	OKS \uparrow	MPS \uparrow	SP \downarrow	GP \downarrow	Float \downarrow	FS \downarrow
PhysPT	0.687	0.497	-	4.789	38.189	4.436
TRAM	0.828	0.667	0.438	19.988	107.432	12.261
TRAM+PhysPT	0.730	0.645	-	7.883	39.379	6.007
TRAM+Ours	0.845	0.687	0.363	0.595	16.956	0.779
GVHMR	0.837	0.704	0.289	9.999	137.969	3.006
GVHMR+PhysPT	0.806	0.685	-	6.616	54.032	5.630
GVHMR+Ours	0.854	0.710	0.120	0.334	14.921	0.717

Table 2. Evaluation of our collected in-the-wild dataset.

Method	SR \uparrow	MPJPE _g \downarrow	MPJPE \downarrow	MPJPE _{pa} \downarrow
UHC	42.91%	86.23	48.91	39.73
PHC+	76.41%	84.86	47.98	39.43
PTM	98.16%	82.13	33.45	26.12

Table 3. Physical transfer ability. The reference motions are from the kungfu subset, following PHC+ in metrics calculation.

Early-Term	Res-F	TTA	Rela-Rwd	OKS \uparrow	MPS \uparrow	SR \uparrow
				0.811	0.673	37%
✓				0.784	0.652	52%
✓	✓			0.823	0.673	61%
✓	✓	✓		0.850	0.706	85%
✓	✓	✓	✓	0.853	0.710	87%

Table 4. Effectiveness of adaptation settings in our PTM.

In-between	Condition		Match-Detect		Metrics		
	mask	kpts	mask	kpts	OKS \uparrow	MPS \uparrow	SR \uparrow
✓					0.802	0.677	78%
✓				✓	0.834	0.699	83%
✓			✓		0.827	0.704	85%
✓		✓	✓		0.845	0.706	87%
✓	✓		✓		0.853	0.710	87%

Table 5. Comparison of different motion correction settings. In-between means whether to use the in-between module to correct the bad frames. The condition tells which signal we used to guide the diffusion in-between process. Match-Detect shows which mismatch detection method is more effective.

fective in addressing flawed motions. The advanced motion imitation method PHC+ is capable of tracking large-scale motion capture datasets but fails on high-difficulty noisy motions. This is attributed to PHC+’s lack of generalization ability for complex movements and its susceptibility to noise in reference motions. In contrast, despite the original motions containing multiple complex motions that are challenging to reproduce in physical space, our method eliminates ground penetration and floating issues while successfully maintaining the original motion patterns. Furthermore, we implement MCM to correct the flawed motion, avoiding the simulation failures caused by flawed motion and ensuring harmony with the video and motion context.

4.6. Ablation Studies

Physical Transfer Ability. We evaluate the simulation capabilities of our proposed PTM using the Kungfu dataset, comparing them against SOTA motion imitation methods, the results are presented in Table 3. Compared to outstanding motion imitation methods UHC and PHC+, our PTM

demonstrates commendable performance in tracking martial arts, achieving a 98% success rate and considerable enhancements across other metrics. These results affirm the superior capability of our methods in motion imitation, particularly in tracking high-difficulty motions. The improvement in metrics is attributed to the relative design tailored for complex motions and the ability of TTA to mitigate the forgetting phenomenon. Previous studies have indicated that motion imitation can suffer from rapid loss of earlier knowledge when attempting to imitate a wide array of motions [33]. In our PTM, the controller’s memory serves as a cornerstone for learning new actions, allowing the optimization of specific data samples without retaining this memory. We aim for the model to proactively explore solutions rather than merely reproducing answers it has memorized.

Effect of RL-TTA Strategy. In Table 4, we conduct an ablation study on various components of the RL-TTA strategy, with experiments carried out on a high-difficulty in-the-wild dataset to demonstrate its effectiveness in handling challenging movements. While the pre-trained controller can track daily motions well, it struggles when facing difficult movements. The reason why success rates increase with early termination is that traditional early termination strategies impose overly strict requirements on humanoids, making it easy to fail when facing poor-quality motion, greatly hindering the learning process. Since high-difficulty motion often involves airborne motions that rely on external apparatuses such as trampolines, the absence of residual forces prevents humanoids from executing these movements. The TTA contributes the most enhancement by simplifying the humanoid’s objectives to a specific action.

Effect of Mask-conditioned Motion Correction. As shown in Table 5, we conduct an ablation study on our MCM, which corrects flawed motions in reference motion. The experiments are performed on a high-difficulty in-the-wild dataset. Experimental results show that our MCM can enhance the simulation success rate and improve 2D similarity by replacing flawed motions that result in simulation failure. Regarding modality selection, we find that human masks outperform 2D keypoints, as masks contain more comprehensive shape and motion information. When facing complex movements, keypoint detection algorithms may misidentify or overlook some joints, while segmentation algorithms exhibit greater stability and only require distinguishing between human foreground and background.

5. Conclusion

This paper introduces a plug-and-play motion restoration method to enhance the physical quality of in-the-wild high-difficulty motions. Our method integrates easily with any video motion capture method, greatly improving the efficiency of obtaining high-quality 3D motions. The MCM accurately corrected the flawed motion in video motion

capture results, while the PTM successfully achieved the physical restoration of high-difficulty in-the-wild motions. Comprehensive experiments showcase our model’s performance and highlight each module’s contributions and impacts. Our work provides valuable insights for future research in this field. The main limitation of our work is that it can only handle single-person motions and is unable to restore closely interactive multi-person movements.

References

- [1] Nuttapon Chentanez, Matthias Müller, Miles Macklin, Viktor Makovychuk, and Stefan Jeschke. Physics-based motion capture imitation with deep reinforcement learning. In *Proceedings of the 11th ACM SIGGRAPH Conference on Motion, Interaction and Games*, pages 1–10, 2018. 3
- [2] Hongsuk Choi, Gyeongsik Moon, Ju Yong Chang, and Kyoung Mu Lee. Beyond static features for temporally consistent 3d human pose and shape from a video. In *Proceedings of the IEEE/CVF conference on computer vision and pattern recognition*, pages 1964–1973, 2021. 2
- [3] Setareh Cohan, Guy Tevet, Daniele Reda, Xue Bin Peng, and Michiel van de Panne. Flexible motion in-betweening with diffusion models. In *ACM SIGGRAPH 2024 Conference Papers*, pages 1–9, 2024. 4
- [4] Jessica Colombel, Vincent Bonnet, David Daney, Raphael Dumas, Antoine Seilles, and François Charpillet. Physically consistent whole-body kinematics assessment based on an rgb-d sensor. application to simple rehabilitation exercises. *Sensors*, 20(10):2848, 2020. 1
- [5] Prafulla Dhariwal and Alexander Nichol. Diffusion models beat gans on image synthesis. *Advances in neural information processing systems*, 34:8780–8794, 2021. 6
- [6] Sai Kumar Dwivedi, Yu Sun, Priyanka Patel, Yao Feng, and Michael J Black. Tokenhmr: Advancing human mesh recovery with a tokenized pose representation. In *Proceedings of the IEEE/CVF Conference on Computer Vision and Pattern Recognition*, pages 1323–1333, 2024. 2
- [7] Zackory Erickson, Vamsee Gangaram, Ariel Kapusta, C Karen Liu, and Charles C Kemp. Assistive gym: A physics simulation framework for assistive robotics. In *2020 IEEE International Conference on Robotics and Automation (ICRA)*, pages 10169–10176. IEEE, 2020. 1
- [8] Levi Fussell, Kevin Bergamin, and Daniel Holden. Super-track: Motion tracking for physically simulated characters using supervised learning. *ACM Transactions on Graphics (TOG)*, 40(6):1–13, 2021. 3
- [9] Erik Gärtner, Mykhaylo Andriluka, Erwin Coumans, and Cristian Sminchisescu. Differentiable dynamics for articulated 3d human motion reconstruction. In *Proceedings of the IEEE/CVF conference on computer vision and pattern recognition*, pages 13190–13200, 2022. 1, 3
- [10] Erik Gärtner, Mykhaylo Andriluka, Hongyi Xu, and Cristian Sminchisescu. Trajectory optimization for physics-based reconstruction of 3d human pose from monocular video. In *Proceedings of the IEEE/CVF Conference on Computer Vision and Pattern Recognition*, pages 13106–13115, 2022. 1, 3
- [11] Yongtao Ge, Wenjia Wang, Yongfan Chen, Hao Chen, and Chunhua Shen. 3d human reconstruction in the wild with synthetic data using generative models. *arXiv preprint arXiv:2403.11111*, 2024. 2
- [12] Kehong Gong, Bingbing Li, Jianfeng Zhang, Tao Wang, Jing Huang, Michael Bi Mi, Jiashi Feng, and Xinchao Wang. Posetriplet: Co-evolving 3d human pose estimation, imitation, and hallucination under self-supervision. In *Proceedings of the IEEE/CVF conference on computer vision and pattern recognition*, pages 11017–11027, 2022. 1, 3
- [13] Kristen Grauman, Andrew Westbury, Lorenzo Torresani, Kris Kitani, Jitendra Malik, Triantafyllos Afouras, Kumar Ashutosh, Vijay Baiyya, Siddhant Bansal, Bikram Boote, et al. Ego-exo4d: Understanding skilled human activity from first-and third-person perspectives. In *Proceedings of the IEEE/CVF Conference on Computer Vision and Pattern Recognition*, pages 19383–19400, 2024. 1
- [14] Jonathan Ho, Ajay Jain, and Pieter Abbeel. Denoising diffusion probabilistic models. *Advances in neural information processing systems*, 33:6840–6851, 2020. 6
- [15] Buzhen Huang, Liang Pan, Yuan Yang, Jingyi Ju, and Yangang Wang. Neural mocon: Neural motion control for physically plausible human motion capture. In *Proceedings of the IEEE/CVF conference on computer vision and pattern recognition*, pages 6417–6426, 2022. 3
- [16] Catalin Ionescu, Dragos Papava, Vlad Olaru, and Cristian Sminchisescu. Human3. 6m: Large scale datasets and predictive methods for 3d human sensing in natural environments. *IEEE transactions on pattern analysis and machine intelligence*, 36(7):1325–1339, 2013. 5
- [17] Angjoo Kanazawa, Jason Y Zhang, Panna Felsen, and Jitendra Malik. Learning 3d human dynamics from video. In *Proceedings of the IEEE/CVF conference on computer vision and pattern recognition*, pages 5614–5623, 2019. 2
- [18] Korrawe Karunratanakul, Konpat Preechakul, Supasorn Suwajanakorn, and Siyu Tang. Gmd: Controllable human motion synthesis via guided diffusion models. *arXiv preprint arXiv:2305.12577*, 3, 2023. 4
- [19] Manuel Kaufmann, Jie Song, Chen Guo, Kaiyue Shen, Tianjian Jiang, Chengcheng Tang, Juan José Zárata, and Otmar Hilliges. Emdb: The electromagnetic database of global 3d human pose and shape in the wild. In *Proceedings of the IEEE/CVF International Conference on Computer Vision*, pages 14632–14643, 2023. 5
- [20] Alexander Kirillov, Eric Mintun, Nikhila Ravi, Hanzi Mao, Chloe Rolland, Laura Gustafson, Tete Xiao, Spencer Whitehead, Alexander C. Berg, Wan-Yen Lo, Piotr Dollár, and Ross Girshick. Segment anything. *arXiv:2304.02643*, 2023. 2, 4
- [21] Muhammed Kocabas, Nikos Athanasiou, and Michael J Black. Vibe: Video inference for human body pose and shape estimation. In *Proceedings of the IEEE/CVF conference on computer vision and pattern recognition*, pages 5253–5263, 2020. 2
- [22] Muhammed Kocabas, Ye Yuan, Pavlo Molchanov, Yunrong Guo, Michael J Black, Otmar Hilliges, Jan Kautz, and Umar Iqbal. Pace: Human and motion estimation from in-the-wild videos. *3DV*, 1(2):7, 2024. 2

- [23] Cuong Le, Viktor Johansson, Manon Kok, and Bastian Wandt. Optimal-state dynamics estimation for physics-based human motion capture from videos. *arXiv preprint arXiv:2410.07795*, 2024. 3
- [24] Jiefeng Li, Siyuan Bian, Chao Xu, Gang Liu, Gang Yu, and Cewu Lu. D & d: Learning human dynamics from dynamic camera. In *European Conference on Computer Vision*, pages 479–496. Springer, 2022. 1, 3
- [25] Ruilong Li, Shan Yang, David A. Ross, and Angjoo Kanazawa. Learn to dance with aist++: Music conditioned 3d dance generation, 2021. 5
- [26] Jing Lin, Ailing Zeng, Shunlin Lu, Yuanhao Cai, Ruimao Zhang, Haoqian Wang, and Lei Zhang. Motion-x: A large-scale 3d expressive whole-body human motion dataset. *Advances in Neural Information Processing Systems*, 2023. 5
- [27] Wenxuan Liu, Xian Zhong, Zhuo Zhou, Kui Jiang, Zheng Wang, and Chia-Wen Lin. Dual-recommendation disentanglement network for view fuzz in action recognition. *IEEE Trans. Image Process.*, 32:2719–2733, 2023. 1
- [28] Matthew Loper, Naureen Mahmood, Javier Romero, Gerard Pons-Moll, and Michael J Black. Smpl: A skinned multi-person linear model. In *Seminal Graphics Papers: Pushing the Boundaries, Volume 2*, pages 851–866. 2023. 2, 3
- [29] Shunlin Lu, Ling-Hao Chen, Ailing Zeng, Jing Lin, Ruimao Zhang, Lei Zhang, and Heung-Yeung Shum. Humantomato: Text-aligned whole-body motion generation. *arXiv preprint arXiv:2310.12978*, 2023. 3
- [30] Zhengyi Luo, S Alireza Golestaneh, and Kris M Kitani. 3d human motion estimation via motion compression and refinement. In *Proceedings of the Asian Conference on Computer Vision*, 2020. 2
- [31] Zhengyi Luo, Ryo Hachiuma, Ye Yuan, and Kris Kitani. Dynamics-regulated kinematic policy for egocentric pose estimation. *Advances in Neural Information Processing Systems*, 34:25019–25032, 2021. 3
- [32] Zhengyi Luo, Shun Iwase, Ye Yuan, and Kris Kitani. Embodied scene-aware human pose estimation. *Advances in Neural Information Processing Systems*, 35:6815–6828, 2022. 1
- [33] Zhengyi Luo, Jinkun Cao, Kris Kitani, Weipeng Xu, et al. Perpetual humanoid control for real-time simulated avatars. In *Proceedings of the IEEE/CVF International Conference on Computer Vision*, pages 10895–10904, 2023. 2, 3, 4, 8
- [34] Zhengyi Luo, Jinkun Cao, Josh Merel, Alexander Winkler, Jing Huang, Kris Kitani, and Weipeng Xu. Universal humanoid motion representations for physics-based control. *arXiv preprint arXiv:2310.04582*, 2023. 3, 6
- [35] Zhengyi Luo, Jiashun Wang, Kangni Liu, Haotian Zhang, Chen Tessler, Jingbo Wang, Ye Yuan, Jinkun Cao, Zihui Lin, Fengyi Wang, et al. Smpolympics: Sports environments for physically simulated humanoids. *arXiv preprint arXiv:2407.00187*, 2024. 3
- [36] Sihan Ma, Qiong Cao, Hongwei Yi, Jing Zhang, and Dacheng Tao. Grammar: Ground-aware motion model for 3d human motion reconstruction. In *Proceedings of the 31st ACM International Conference on Multimedia*, pages 2817–2828, 2023. 2
- [37] Naureen Mahmood, Nima Ghorbani, Nikolaus F Troje, Gerard Pons-Moll, and Michael J Black. Amass: Archive of motion capture as surface shapes. In *Proceedings of the IEEE/CVF international conference on computer vision*, pages 5442–5451, 2019. 5
- [38] Dushyant Mehta, Srinath Sridhar, Oleksandr Sotnychenko, Helge Rhodin, Mohammad Shafiei, Hans-Peter Seidel, Weipeng Xu, Dan Casas, and Christian Theobalt. Vnect: Real-time 3d human pose estimation with a single rgb camera. *Acm transactions on graphics (tog)*, 36(4):1–14, 2017. 1
- [39] Josh Merel, Saran Tunyasuvunakool, Arun Ahuja, Yuval Tassa, Leonard Hasenclever, Vu Pham, Tom Erez, Greg Wayne, and Nicolas Heess. Catch & carry: reusable neural controllers for vision-guided whole-body tasks. *ACM Transactions on Graphics (TOG)*, 39(4):39–1, 2020. 3
- [40] Xue Bin Peng, Glen Berseth, KangKang Yin, and Michiel Van De Panne. Deeploco: Dynamic locomotion skills using hierarchical deep reinforcement learning. *Acm transactions on graphics (tog)*, 36(4):1–13, 2017.
- [41] Xue Bin Peng, Pieter Abbeel, Sergey Levine, and Michiel Van de Panne. Deepmimic: Example-guided deep reinforcement learning of physics-based character skills. *ACM Transactions On Graphics (TOG)*, 37(4):1–14, 2018. 4
- [42] Xue Bin Peng, Michael Chang, Grace Zhang, Pieter Abbeel, and Sergey Levine. Mcp: Learning composable hierarchical control with multiplicative compositional policies. *Advances in neural information processing systems*, 32, 2019.
- [43] Xue Bin Peng, Ze Ma, Pieter Abbeel, Sergey Levine, and Angjoo Kanazawa. Amp: Adversarial motion priors for stylized physics-based character control. *ACM Transactions on Graphics (ToG)*, 40(4):1–20, 2021. 4
- [44] Xue Bin Peng, Yunrong Guo, Lina Halper, Sergey Levine, and Sanja Fidler. Ase: Large-scale reusable adversarial skill embeddings for physically simulated characters. *ACM Transactions On Graphics (TOG)*, 41(4):1–17, 2022. 3
- [45] Davis Rempe, Tolga Birdal, Aaron Hertzmann, Jimei Yang, Srinath Sridhar, and Leonidas J Guibas. Humor: 3d human motion model for robust pose estimation. In *Proceedings of the IEEE/CVF international conference on computer vision*, pages 11488–11499, 2021. 2
- [46] Davis Rempe, Zhengyi Luo, Xue Bin Peng, Ye Yuan, Kris Kitani, Karsten Kreis, Sanja Fidler, and Or Litany. Trace and pace: Controllable pedestrian animation via guided trajectory diffusion. In *Proceedings of the IEEE/CVF Conference on Computer Vision and Pattern Recognition*, pages 13756–13766, 2023. 1
- [47] Jiawei Ren, Cunjun Yu, Siwei Chen, Xiao Ma, Liang Pan, and Ziwei Liu. Diffmimic: Efficient motion mimicking with differentiable physics. *arXiv preprint arXiv:2304.03274*, 2023. 3
- [48] John Schulman, Filip Wolski, Prafulla Dhariwal, Alec Radford, and Oleg Klimov. Proximal policy optimization algorithms. *arXiv preprint arXiv:1707.06347*, 2017. 4
- [49] Xiaolong Shen, Zongxin Yang, Xiaohan Wang, Jianxin Ma, Chang Zhou, and Yi Yang. Global-to-local modeling for video-based 3d human pose and shape estimation. In *Proceedings of the IEEE/CVF Conference on Computer Vision and Pattern Recognition*, pages 8887–8896, 2023. 2

- [50] Zehong Shen, Huaijin Pi, Yan Xia, Zhi Cen, Sida Peng, Zechen Hu, Hujun Bao, Ruizhen Hu, and Xiaowei Zhou. World-grounded human motion recovery via gravity-view coordinates. In *SIGGRAPH Asia Conference Proceedings*, 2024. 2, 5, 6, 7
- [51] Soshi Shimada, Vladislav Golyanik, Weipeng Xu, and Christian Theobalt. Physcap: Physically plausible monocular 3d motion capture in real time. *ACM Transactions on Graphics (ToG)*, 39(6):1–16, 2020. 1, 3
- [52] Soshi Shimada, Vladislav Golyanik, Weipeng Xu, Patrick Pérez, and Christian Theobalt. Neural monocular 3d human motion capture with physical awareness. *ACM Transactions on Graphics (ToG)*, 40(4):1–15, 2021. 3
- [53] Soyong Shin, Juyong Kim, Eni Halilaj, and Michael J Black. Wham: Reconstructing world-grounded humans with accurate 3d motion. In *Proceedings of the IEEE/CVF Conference on Computer Vision and Pattern Recognition*, pages 2070–2080, 2024. 2, 5
- [54] Yu Sun, Yun Ye, Wu Liu, Wenpeng Gao, Yili Fu, and Tao Mei. Human mesh recovery from monocular images via a skeleton-disentangled representation. In *Proceedings of the IEEE/CVF international conference on computer vision*, pages 5349–5358, 2019. 2
- [55] Yu Sun, Qian Bao, Wu Liu, Tao Mei, and Michael J Black. Trace: 5d temporal regression of avatars with dynamic cameras in 3d environments. In *Proceedings of the IEEE/CVF Conference on Computer Vision and Pattern Recognition*, pages 8856–8866, 2023. 2
- [56] Zachary Teed and Jia Deng. Droid-slam: Deep visual slam for monocular, stereo, and rgb-d cameras. *Advances in neural information processing systems*, 34:16558–16569, 2021. 2
- [57] Zachary Teed, Lahav Lipson, and Jia Deng. Deep patch visual odometry. *Advances in Neural Information Processing Systems*, 36, 2024. 2
- [58] Yating Tian, Hongwen Zhang, Yebin Liu, and Limin Wang. Recovering 3d human mesh from monocular images: A survey. *IEEE transactions on pattern analysis and machine intelligence*, 2023. 2
- [59] Shashank Tripathi, Lea Müller, Chun-Hao P Huang, Omid Taheri, Michael J Black, and Dimitrios Tzionas. 3d human pose estimation via intuitive physics. In *Proceedings of the IEEE/CVF conference on computer vision and pattern recognition*, pages 4713–4725, 2023. 1, 3
- [60] Shuhei Tsuchida, Satoru Fukayama, Masahiro Hamasaki, and Masataka Goto. Aist dance video database: Multi-genre, multi-dancer, and multi-camera database for dance information processing. In *Proceedings of the 20th International Society for Music Information Retrieval Conference, ISMIR 2019*, pages 501–510, Delft, Netherlands, 2019. 5
- [61] Nolan Wagener, Andrey Kolobov, Felipe Vieira Frujeri, Ricky Loynd, Ching-An Cheng, and Matthew Hausknecht. Mocapact: A multi-task dataset for simulated humanoid control. *Advances in Neural Information Processing Systems*, 35:35418–35431, 2022. 3
- [62] Jingbo Wang, Ye Yuan, Zhengyi Luo, Kevin Xie, Dahua Lin, Umar Iqbal, Sanja Fidler, and Sameh Khamis. Learning human dynamics in autonomous driving scenarios. In *Proceedings of the IEEE/CVF International Conference on Computer Vision*, pages 20796–20806, 2023. 1
- [63] Jingbo Wang, Zhengyi Luo, Ye Yuan, Yixuan Li, and Bo Dai. Pacer+: On-demand pedestrian animation controller in driving scenarios. In *Proceedings of the IEEE/CVF Conference on Computer Vision and Pattern Recognition*, pages 718–728, 2024. 3
- [64] Jiong Wang, Fengyu Yang, Bingliang Li, Wenbo Gou, Danqi Yan, Ailing Zeng, Yijun Gao, Junle Wang, Yanqing Jing, and Ruimao Zhang. Freeman: Towards benchmarking 3d human pose estimation under real-world conditions. In *Proceedings of the IEEE/CVF Conference on Computer Vision and Pattern Recognition*, pages 21978–21988, 2024. 1
- [65] Tingwu Wang, Yunrong Guo, Maria Shugrina, and Sanja Fidler. Unicon: Universal neural controller for physics-based character motion. *arXiv preprint arXiv:2011.15119*, 2020. 3
- [66] Yinhuai Wang, Qihan Zhao, Runyi Yu, Ailing Zeng, Jing Lin, Zhengyi Luo, Hok Wai Tsui, Jiwen Yu, Xiu Li, Qifeng Chen, et al. Skillmimic: Learning reusable basketball skills from demonstrations. *arXiv preprint arXiv:2408.15270*, 2024. 3
- [67] Yufu Wang, Ziyun Wang, Lingjie Liu, and Kostas Daniilidis. Tram: Global trajectory and motion of 3d humans from in-the-wild videos. In *European Conference on Computer Vision*, pages 467–487. Springer, 2025. 2, 5, 6, 7
- [68] Alexander Winkler, Jungdam Won, and Yuting Ye. Questsim: Human motion tracking from sparse sensors with simulated avatars. In *SIGGRAPH Asia 2022 Conference Papers*, pages 1–8, 2022. 3
- [69] Jungdam Won, Deepak Gopinath, and Jessica Hodgins. A scalable approach to control diverse behaviors for physically simulated characters. *ACM Transactions on Graphics (TOG)*, 39(4):33–1, 2020. 3
- [70] Kevin Xie, Tingwu Wang, Umar Iqbal, Yunrong Guo, Sanja Fidler, and Florian Shkurti. Physics-based human motion estimation and synthesis from videos. In *Proceedings of the IEEE/CVF International Conference on Computer Vision*, pages 11532–11541, 2021. 1, 3
- [71] Vickie Ye, Georgios Pavlakos, Jitendra Malik, and Angjoo Kanazawa. Decoupling human and camera motion from videos in the wild. In *Proceedings of the IEEE/CVF conference on computer vision and pattern recognition*, pages 21222–21232, 2023. 2
- [72] Ye Yuan and Kris Kitani. Residual force control for agile human behavior imitation and extended motion synthesis. *Advances in Neural Information Processing Systems*, 33: 21763–21774, 2020. 3, 5
- [73] Ye Yuan, Shih-En Wei, Tomas Simon, Kris Kitani, and Jason Saragih. Simpoe: Simulated character control for 3d human pose estimation. In *Proceedings of the IEEE/CVF conference on computer vision and pattern recognition*, pages 7159–7169, 2021. 1, 3
- [74] Ye Yuan, Jiaming Song, Umar Iqbal, Arash Vahdat, and Jan Kautz. Physdiff: Physics-guided human motion diffusion model. In *Proceedings of the IEEE/CVF international conference on computer vision*, pages 16010–16021, 2023. 4
- [75] Siwei Zhang, Yan Zhang, Federica Bogo, Marc Pollefeys, and Siyu Tang. Learning motion priors for 4d human body

- capture in 3d scenes. In *Proceedings of the IEEE/CVF International Conference on Computer Vision*, pages 11343–11353, 2021. [3](#)
- [76] Yufei Zhang, Jeffrey O Kephart, Zijun Cui, and Qiang Ji. Physpt: Physics-aware pretrained transformer for estimating human dynamics from monocular videos. In *Proceedings of the IEEE/CVF Conference on Computer Vision and Pattern Recognition*, pages 2305–2317, 2024. [3](#), [6](#), [7](#)
- [77] Youliang Zhang, Wenxuan Liu, Danni Xu, Zhuo Zhou, and Zheng Wang. Bi-causal: Group activity recognition via bidirectional causality. In *Proceedings of the IEEE/CVF Conference on Computer Vision and Pattern Recognition*, pages 1450–1459, 2024. [1](#)
- [78] Yuxiang Zhang, Hongwen Zhang, Liangxiao Hu, Jiajun Zhang, Hongwei Yi, Shengping Zhang, and Yebin Liu. Proxycap: Real-time monocular full-body capture in world space via human-centric proxy-to-motion learning. In *Proceedings of the IEEE/CVF Conference on Computer Vision and Pattern Recognition*, pages 1954–1964, 2024. [3](#)
- [79] Yi Zhou, Connelly Barnes, Jingwan Lu, Jimei Yang, and Hao Li. On the continuity of rotation representations in neural networks. In *Proceedings of the IEEE/CVF conference on computer vision and pattern recognition*, pages 5745–5753, 2019. [3](#)